

Low-temperature lattice thermal conductivity of heavily deformed metallic alloys

F. L. Madarasz

Universal Energy Systems, Dayton, Ohio 45432

F. Szmulowicz

University of Dayton Research Institute, Dayton, Ohio 45469

(Received 17 January 1983)

Lattice thermal conductivity in Cu-Al alloys is calculated for the first time within a two-dimensional formalism involving the scattering of phonons by strain fields of finite spatial extent around randomly oriented dislocations of edge and screw character. For the finite strain fields, scattering widths indicate that long-wavelength phonons scatter very weakly. In addition to phonon scattering by the strain field around the dislocation, phonon-electron scattering is included to obtain the overall phonon relaxation rate. Comparison is made between the calculated results and measurements on the commercial alloy Evanohm. Evanohm has a very high residual resistivity and thus possesses a low electronic thermal conductivity. Therefore, the phonon contribution to the thermal conductivity may be unambiguously identified for this alloy unlike the situation encountered for most other alloys at very low temperatures. The calculated lattice thermal conductivity is found to depart from the usual T^2 dependence in general agreement with the measurements on Evanohm.

I. INTRODUCTION

Dense arrays of dislocations arrange themselves in such a manner as to minimize the free energy. In doing so, the strain fields of individual dislocations tend to cancel each other resulting in a finite average cutoff radius for the strain field about each dislocation. This average cutoff radius R may be related to the density of dislocations.¹ It is to be expected that for phonon wavelengths large compared to R scattering will be weak. This should happen at very low temperatures. But, as the temperature is increased, phonon wavelengths become shorter and scattering becomes stronger until, finally, phonon wavelengths become small compared to R and infinite strain-field scattering results. In the latter case, lattice thermal conductivity K_g varies with temperatures as T^2 (Ref. 2).

The above model was first proposed by Ackerman and Klemens,³ who predicted that the finite range of the strain field around a dislocation leads to a decrease of the thermal resistivity below some temperature which is determined by the dislocation density.

A departure from $K_g \propto T^2$ was seen in all the deformed alloys investigated by Linz *et al.*,⁴ but was overshadowed in the alloys of low residual resistivity by another anomaly, present in all alloys (both annealed and deformed), which also seemed to increase K_g below 0.7 K. Only in one alloy, Evanohm, which has a very high residual resistivity, did this additional anomaly seem to be unimportant, and did K_g follow approximately the predictions of Ackerman and Klemens.³

Linz *et al.*⁴ were not able to explain this discrepancy, though they suggested that it was due to mobile dislocations. This left in abeyance the question of why dislocations were less mobile in Evanohm. Furthermore, Anderson⁵ pointed out that their anomalous K_g varied too rapidly around 0.7 K to be explained by any phonon scattering mechanism.

It seems more likely that the anomaly is due to a

measuring error in the total thermal conductivity K_{tot} . Any such error would be multiplied since the Lorenz number was used to calculate the electronic thermal conductivity K_e , and K_g was found from $K_{\text{tot}} - K_e$. Indeed the anomaly is not present in Evanohm, simply because for this alloy K_e is small, while in the other alloys $K_{\text{tot}} - K_e$ is only a small fraction of K_{tot} . It now appears possible that it was due to a small error in the vapor pressure thermometry caused by an incipient thermomolecular effect at the lowest of temperatures.⁶

For this reason, the effect of Ackerman and Klemens was only clearly seen in Evanohm, but may well have been present in all the heavily deformed alloys. Cu-10 at. % Al, which has the next highest residual resistivity, exhibits this anomalous behavior below 0.7 K. However, above 0.7 K, K_g behaves similar to K_g for Evanohm but with an additional slight bowing between 2-3 K. This bowing was explained by Madarasz and Klemens⁷ who employed a resonant scattering model.

The finite strain-field model of phonon scattering by dislocations does appear to be a valid one for Cu-10 at. % Al. The original theoretical work of Ackerman and Klemens³ did address this alloy system. However, the phonon scattering by a dislocation was treated as a three-dimensional scattering problem. In particular, Eq. (11) of Ref. 3 is only appropriate for a three-dimensional spherically symmetric scattering center.⁸ As discussed by Ziman,⁸ though, phonon scattering by a dislocation is a two-dimensional scattering problem.

In the present paper the formalism of Ackerman and Klemens is applied in the two-dimensional regime. Also, we have extended the calculation to include the effects of an edge dislocation with a finite cutoff radius. The original work³ only considered screw dislocations. An additional feature of the present work is the averaging of phonon wave vectors onto the plane of scattering.

In Sec. II we present the theory of phonon-dislocation scattering by edge and screw dislocations and calculate

their scattering widths. These results are then applied to the problem of lattice thermal conductivity of copper alloys in Sec. III. Additionally in Sec. III we compare the results of our calculation with those of Ackerman and Klemens. Significant differences are found. We further discuss the dislocation dipole model and the difficulties in obtaining data on Cu-Al alloys at low temperatures which may be directly compared with the present model's predictions of lattice thermal conductivity. A summary is given in Sec. IV.

II. THEORY

In this section we follow, in general, the approach to phonon-dislocation scattering as prescribed by Ziman.⁸ Just as a photon's velocity is varied when traveling a medium of changing index of refraction, so too is the phonon's velocity varied when traveling through a strained region. Thus we may write the fractional change in phonon velocity c_s , when $\delta c_s/c_s \ll 1$, as

$$\delta c_s/c_s = \gamma \epsilon. \quad (2.1)$$

Here, γ is the Grüneisen constant and ϵ is representative of the component (s) of the strain tensor which produces the phonon scattering. Since the energy of a phonon with wave vector \vec{q}'_0 is $\hbar \vec{q}'_0 c_s$, we may, with the aid of Eq. (2.1), write the perturbation energy density U , due to an element of the strain field ϵ_{ij} , as

$$U(\epsilon_{ij}) = \gamma \hbar \vec{q}'_0 c_s \epsilon_{ij}, \quad (2.2)$$

where \hbar is Planck's constant divided by 2π .

The scattering from a phonon state of wave vector \vec{q}_0 to \vec{q}_s is shown graphically in Fig. 1 where the dislocation axis is along the z axis. Because of cylindrical symmetry and the assumption of elastic scattering, the z component of the wave vector is conserved and the problem of phonon scattering by a dislocation reduces to a purely two-dimensional process in which scattering takes place between \vec{q}'_0 to \vec{q}'_s in the xy plane. The prime indicates that the scattering is between the components of \vec{q}_0 and \vec{q}_s projected onto the xy plane, i.e., $q'_0 = q'_s = q_0 \sin \theta_0$.

The transition matrix in the first Born approximation due to an element of the strain field is given by

$$\langle \vec{q}'_s | U(\epsilon_{ij}) | \vec{q}'_0 \rangle = \frac{1}{A_\rho} \int_0^{2\pi} \int_{r_0}^R U(\epsilon_{ij}) e^{i \vec{Q}' \cdot \vec{\rho}} \rho d\rho d\phi. \quad (2.3)$$

In this equation A_ρ is the area inside a circle of radius $\rho = R$ lying in the xy plane in which the transition from \vec{q}'_0 to \vec{q}'_s takes place, and $\vec{Q}' = \vec{q}'_0 - \vec{q}'_s$. The polar coordinates (ρ, ϕ) in the xy plane label the field vector $\vec{\rho}$ of the dislocation strain field. The relationship between $\vec{\rho}$ and \vec{Q}' is shown in Fig. 2. r_0 and R are dislocation core radius and the strain-field—cutoff radius, respectively.

The elements of the strain tensor for both screw and edge dislocations are given by Nabarro.⁹ For the screw dislocation they are

$$\epsilon_{xz} = \epsilon_{zx} = \frac{-b \sin \phi}{4\pi \rho}, \quad (2.4a)$$

$$\epsilon_{yz} = \epsilon_{zy} = \frac{b \cos \phi}{4\pi \rho}, \quad (2.4b)$$

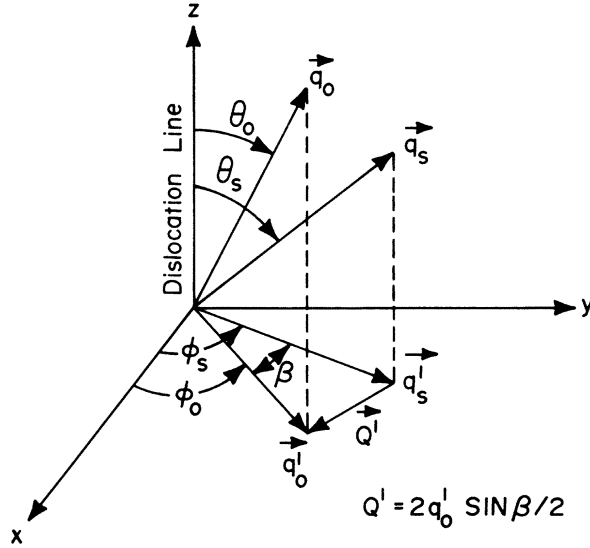


FIG. 1. Scattering diagram of the elastic scattering from an initial phonon state of wave vector \vec{q}_0 to a final phonon state of wave vector \vec{q}_s by the strain field of a dislocation reduces to a two-dimensional problem where scattering takes place between \vec{q}'_0 and \vec{q}'_s in a plane perpendicular to the line of the dislocation. Since the z component of \vec{q}_0 is conserved $q'_0 = q_0 \sin \theta_0 = q'_s$ and $Q' = 2q'_0 \sin(\beta/2)$.

and for the edge dislocation they are

$$\epsilon_{xx} = \frac{-b}{4\pi(1-\nu)\rho} [(1-2\nu)\sin\phi + 2\sin\phi \cos^2\phi], \quad (2.5a)$$

$$\epsilon_{yy} = \frac{-b}{4\pi(1-\nu)\rho} [(1-2\nu)\sin\phi - 2\sin\phi \cos^2\phi], \quad (2.5b)$$

$$\epsilon_{xy} = \epsilon_{yx} = \frac{b}{4\pi(1-\nu)\rho} [\cos\phi(\cos^2\phi - \sin^2\phi)], \quad (2.5c)$$

where b is the magnitude of the Burgers vector and ν is the Poisson ratio. The above expressions assume the xz plane to be the slip plane and, in the case of the edge dislocation, \vec{b} to lie along the x axis.

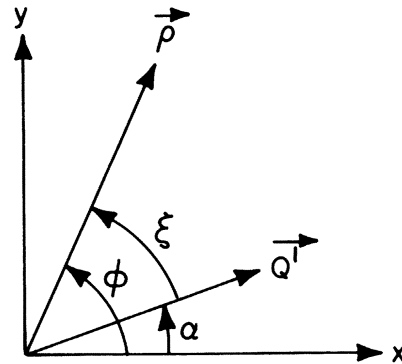


FIG. 2. Angles which label the strain-field position vector $\vec{\rho}$, the scattering vector \vec{Q}' , and their relationship $\phi = \xi + \alpha$.

Let us now consider the calculation of Eq. (2.3), the transition matrix for each strain component. Consider first the elements due to the strain field of a screw dislocation. Because there is no preferred direction of the Burgers vector in the plane for this case, we may rotate the coordinate system in Fig. 2 so that \vec{Q}' is parallel to the x axis and $\alpha=0$, resulting in $\phi=\xi$. Then the transition matrix for the ϵ_{yz} component of the strain field becomes¹⁰

$$\begin{aligned} \langle \vec{q}'_s | U(\epsilon_{yz}) | \vec{q}'_0 \rangle &= \frac{\gamma b \hbar q'_0 c_s}{4\pi A_\rho} \\ &\times \int_0^{2\pi} \int_{r_0}^R \cos\phi \exp(iQ'\rho \cos\phi) \\ &\times d\rho d\phi. \end{aligned} \quad (2.6)$$

Doing the ρ integration first results in

$$\langle \vec{q}'_s | U(\epsilon_{yz}) | \vec{q}'_0 \rangle = \frac{\gamma b \hbar q'_0 c_s}{4\pi i Q' A_\rho} \int_0^{2\pi} \exp(iQ'\rho \cos\phi) \Big|_{r_0}^R d\phi. \quad (2.7)$$

The integral definition of J_0 , the Bessel function of order zero, is

$$J_0(x) = \frac{1}{2\pi} \int_0^{2\pi} \exp(ix \cos\phi) d\phi. \quad (2.8)$$

With this definition, Eq. (2.7) takes the form

$$\langle \vec{q}'_s | U(\epsilon_{yz}) | \vec{q}'_0 \rangle = \frac{\gamma b \hbar q'_0 c_s}{2i Q' A_\rho} J_0(Q'\rho) \Big|_{r_0}^R. \quad (2.9)$$

When performing the same integration for ϵ_{xx} , Eq. (2.7) would contain a $\tan\phi$ in the integrand. Integration over the full angular range of 2π would then yield zero. Therefore, only the symmetric part of the strain field need be considered.

The matrix elements for the strain tensor elements of an edge dislocation are not as straightforward to evaluate. In this case the Burgers vector does have a preferred direction and a rotation of the coordinate system of Fig. 2, such that $\alpha=0$, cannot be done. We must include both the α and ξ angular dependences in the integration process with the constraint $\phi=\xi+\alpha$. The details of these calculations are quite lengthy and involved, and will not be given. However, the results are as follows:

$$\begin{aligned} \langle \vec{q}'_s | U(\epsilon_{xx}) | \vec{q}'_0 \rangle &= \frac{-\gamma b \hbar q'_0 c_s}{fi Q' A_\rho} \\ &\times \left[HJ_0(Q'\rho) - 2I \frac{J_1(Q'\rho)}{Q'\rho} \right]_{r_0}^R, \end{aligned} \quad (2.10)$$

where

$$H = [(1-2\nu) + 2\cos^2\alpha] \sin\alpha, \quad (2.11)$$

$$I = (3\cos^2\alpha - \sin^2\alpha) \sin\alpha, \quad (2.12)$$

$$f = 2(1-\nu), \quad (2.13)$$

and J_1 is the Bessel function of order 1,

$$\begin{aligned} \langle \vec{q}'_s | U(\epsilon_{yy}) | \vec{q}'_0 \rangle &= \frac{-\gamma b \hbar q'_0 c_s}{fi Q' A_\rho} \\ &\times \left[KJ_0(Q'\rho) + 2I \frac{J_1(Q'\rho)}{Q'\rho} \right]_{r_0}^R, \end{aligned} \quad (2.14)$$

where

$$K = [(1-2\nu) - 2\cos^2\alpha] \sin\alpha, \quad (2.15)$$

$$\begin{aligned} \langle \vec{q}'_s | U(\epsilon_{xy}) | \vec{q}'_0 \rangle &= \frac{\gamma \hbar q'_0 c_s}{fi Q' A_\rho} \\ &\times \left[(M-1)J_0(Q'\rho) + 2N \frac{J_1(Q'\rho)}{Q'\rho} \right]_{r_0}^R, \end{aligned} \quad (2.16)$$

where

$$M = 2\cos^3\alpha - \cos\alpha + 1, \quad (2.17)$$

and

$$N = (3\sin^2\alpha - \cos^2\alpha) \cos\alpha. \quad (2.18)$$

We are now in a position to calculate differential scattering widths for a screw and an edge dislocation. In general, the differential scattering width is given by the expression

$$\frac{d\sigma}{d\beta} = \frac{W_{\vec{q}'_0 \rightarrow \vec{q}'_s}}{(c_s/A_\rho) d\beta}. \quad (2.19)$$

The angle β is defined in Fig. 1; it is the scattering angle between \vec{q}'_0 and \vec{q}'_s . The transition rate $W_{\vec{q}'_0 \rightarrow \vec{q}'_s}$ is given by¹¹

$$W_{\vec{q}'_0 \rightarrow \vec{q}'_s} = \frac{2\pi}{\hbar} [2 |\langle \vec{q}'_s | U(\epsilon_{xx}) | \vec{q}'_0 \rangle|^2] \rho_f, \quad (2.20)$$

for the screw dislocation, and by

$$\begin{aligned} W_{\vec{q}'_0 \rightarrow \vec{q}'_s} &= \frac{2\pi}{\hbar} [|\langle \vec{q}'_s | U(\epsilon_{xx}) | \vec{q}'_0 \rangle|^2 \\ &+ |\langle \vec{q}'_s | U(\epsilon_{yy}) | \vec{q}'_0 \rangle|^2 \\ &+ 2 |\langle \vec{q}'_s | U(\epsilon_{xy}) | \vec{q}'_0 \rangle|^2] \rho_f, \end{aligned} \quad (2.21)$$

for the edge dislocation. The factor of 2 within the brackets of (2.20) and (2.21) arises because the strain tensor is symmetric and there must be another equal contribution to the scattering for each off-diagonal element. Also, in the above expressions ρ_f is the density of final scattering states given by Ziman⁸ as

$$\rho_f = \frac{A_\rho q'_0}{4\pi^2 \hbar c_s} d\beta. \quad (2.22)$$

Combining Eqs. (2.9), (2.19), and (2.20), and Eqs. (2.10), (2.14), (2.16), (2.19), (2.21), and (2.22) yields

$$\frac{d\sigma_S}{d\beta} = \frac{\gamma^2 b^2 q'_0}{8\pi(2\sin^2\beta/2)} [1 - 2J_0(Q'R) + J_0^2(Q'R)], \quad (2.23)$$

$$\frac{d\sigma_E}{d\beta} = \frac{\gamma^2 b^2 q'_0}{f^2 4\pi(2\sin^2\beta/2)} \left[A + BJ_0(Q'R) + CJ_0^2(Q'R) + D \frac{J_1(Q'R)}{Q'R} + E \frac{J_1^2(Q'R)}{(Q'R)^2} + F \frac{J_0(Q'R)J_1(Q'R)}{Q'R} \right], \quad (2.24)$$

for screw and edge dislocations, respectively. To obtain the above expressions we have used the fact that $Q' = 2q'_0 \sin\beta/2$ and the approximations $J_0(Q'r_0) \rightarrow 1$, $J_1(Q'r_0)/Q'r_0 \rightarrow \frac{1}{2}$ when $Q'r_0 \ll 1$. This should be especially true at low temperatures where q'_0 is small. The core radius is on the order of a lattice constant. The forms of the coefficients in Eq. (2.24) are as follows:

$$A = (H - I)^2 + (K + I)^2 + 2[(M - 1) + N]^2, \quad (2.25a)$$

$$B = 2\{(HI - H^2) - (KI + K^2) - 2[N(M - 1) + (M - 1)^2]\}, \quad (2.25b)$$

$$C = H^2 + K^2 + 2(M - 1)^2, \quad (2.25c)$$

$$D = 4\{2(HI - I^2) - 2(KI + I^2) - 2[N(M - 1) + N^2]\}, \quad (2.25d)$$

$$E = 8(I^2 + N^2), \quad (2.25e)$$

$$F = -4[HI - KI - N(M - 1)]. \quad (2.25f)$$

What is of interest in transport problems is the total weighted scattering width. The differential scattering width is first weighted by a factor which measures the rel-

ative change in the component of phonon velocity along the initial direction of motion and then integrated over the scattering angle, viz.,

$$\sigma = \int_{-\pi}^{+\pi} \left[1 - \frac{n_s}{n_0} \right] \frac{d\sigma}{d\beta} d\beta, \quad (2.26)$$

where $n_s \propto \vec{q}'_s \cdot \vec{\nabla}T$ and $n_0 \propto \vec{q}'_0 \cdot \vec{\nabla}T$, and $\vec{\nabla}T$ is the temperature gradient. This weighting factor is quite complicated and possesses several singularities. The difficulties with it arise because of the cylindrical symmetry of the problem. They are discussed at some length by Carruthers¹² and, following him, we approximate the weighting factor $1 - n_s/n_0$ by $1 - \cos\beta$. Thus inserting Eq. (2.23) and Eq. (2.24) into Eq. (2.26) and carrying out the integration we get

$$\sigma_S = \frac{\gamma^2 b^2 q'_0}{4} \left[1 - 2J_0^2(q'_0 R) + \frac{1}{2\pi} \int_{-\pi}^{+\pi} J_0^2(Q'R) d\beta \right] \quad (2.27)$$

and

$$\begin{aligned} \sigma_E = \frac{\gamma^2 b^2 q'_0}{4\pi f^2} & \left[2\pi A + 2\pi B J_0^2(q'_0 R) + C \int_{-\pi}^{+\pi} J_0^2(Q'R) d\beta + \frac{D}{2q'_0 R} \int_{-\pi}^{+\pi} \frac{J_1(Q'R)}{\sin(\beta/2)} d\beta \right. \\ & \left. + \frac{E}{(2q'_0 R)^2} \int_{-\pi}^{+\pi} \frac{J_1^2(Q'R)}{\sin^2(\beta/2)} d\beta + \frac{F}{2q'_0 R} \int_{-\pi}^{+\pi} \frac{J_0(Q'R)J_1(Q'R)}{\sin(\beta/2)} d\beta \right]. \quad (2.28) \end{aligned}$$

We have found that only the J_0 terms of Eqs. (2.23) and (2.24) could be integrated analytically. All the other terms involving Bessel functions had to be integrated numerically. However, there were two added difficulties which we considered when evaluating (2.27) and (2.28). First, both scattering widths are functionally dependent on $q'_0 = q_0 \sin\theta_0$, the projection of q_0 onto the xy plane. We therefore averaged these expressions over θ_0 , which gave us double integrals to evaluate. Of course, for the first term of each expression the averaging was straightforward and gave a multiplicative factor of $\pi/4$. Second, the coefficients in the expression for the scattering width of an edge dislocation are functionally dependent on the angle α and, hence, we had to average this expression over α . When this was done the numerical values obtained were the following:

$$\begin{aligned} A &= \frac{10}{9}, \quad B = -\frac{2}{9}, \\ C &= \frac{10}{9}, \quad D = -4, \\ E &= 8, \quad F = -4. \end{aligned} \quad (2.29)$$

In the next section we will apply the results of our scattering width calculations to the problem of lattice thermal conductivity of copper alloys.

III. THERMAL CONDUCTIVITY

For an isotropic Debye continuum the lattice thermal conductivity is given by

$$K_g = \frac{k_B \omega_D^3}{2\pi^2 c_s} \left[\frac{T}{\Theta_D} \right]^3 \int_0^{\Theta_D/T} \frac{x^4 e^x}{(e^x - 1)^2} \tau(\omega) dx, \quad (3.1)$$

where $x = \hbar\omega/k_B T$, Θ_D is the Debye temperature, ω_D is the Debye frequency, k_B is the Boltzmann constant, and τ is the total relaxation time.

At very low temperatures the total relaxation time is made up of contributions from phonon-electron scattering τ_{ph-e} , phonon-screw dislocation interaction τ_S , and phonon-edge dislocation interaction τ_E . At these temperatures umklapp processes are very weak and may be neglected. Normal processes may also be disregarded

since none of the scattering mechanisms being considered are strongly dependent on frequency. Thus the total relaxation rate is

$$\frac{1}{\tau} = \frac{1}{\tau_{\text{ph-e}}} + \frac{1}{\tau_E} + \frac{1}{\tau_S} . \quad (3.2)$$

The phonon-electron relaxation time is directly proportional to the wavelength² and may be written as

$$\tau_{\text{ph-e}} = E/q_0 . \quad (3.3)$$

For copper alloys the interaction parameter $E = 1.12 \times 10^{-2} \text{ sec/cm}^7$.

The relaxation times for the anharmonic dislocation scattering are related to the scattering widths of Eqs. (2.27) and (2.28) by

$$\tau_S = 1/N_S \sigma_S c_s \quad (3.4a)$$

and

$$\tau_E = 1/N_E \sigma_E c_s . \quad (3.4b)$$

Again, both σ_S and σ_E must be evaluated numerically for each q_0 . In addition, these quantities were averaged over values of q_0 projected onto the xy plane. The speed of sound c_s is a spherically averaged speed and has the value of $c_s = 2.78 \times 10^5 \text{ cm/sec}$ for copper. N_E and N_S are the densities of edge and screw dislocations. The units associated with N are length of dislocation per unit volume of crystal, i.e., cm^{-2} .

In copper alloys edge dislocations are predominant.¹³ We thus assume there are twice as many edge as screw dislocations, as would be the case in which the Burgers vector is randomly oriented with respect to the dislocation line. In this case $N_E = \frac{2}{3} N_d$ and $N_S = \frac{1}{3} N_d$ are substituted in Eqs. (3.4a) and (3.4b), respectively. Here N_d is the total dislocation density.

Additionally, in Cu-Al alloys, solute atoms tend to cluster about edge dislocations in an attempt to relax its strain field forming the so-called Cottrell atmospheres. These atmospheres are themselves capable of scattering phonons.^{4,14,15} We further assume, then, that the strain-field scattering by an edge dislocation will be enhanced by a factor of 2. This is in rough accord with observation.¹⁵

With the above relaxation rates, and Eq. (3.1), we have calculated theoretical values of lattice thermal conductivity. Figure 3 illustrates the effect of having either all edge or all screw dislocations with finite strain field present. Both curves were calculated for a dislocation density of $N_d = 4.5 \times 10^{11} \text{ cm}^{-2}$. Despite the complexity of the edge scattering width, Eq. (2.28), as compared to that of the screw dislocation, Eq. (2.27), both curves exhibit very similar shapes. The main difference appears to be in the relative strengths of scattering.

If phonons are scattered both by edge and screw dislocations, the curves in Fig. 4 are the result. These curves were calculated based on a ratio of two edge to one screw dislocation as discussed earlier. For comparison, we have calculated several curves for different dislocation densities as indicated on the figure. Equivalently, these curves were calculated for a different strain-field-cutoff radius. The relationship between the two quantities is given by Kocks and Scattergood¹; it is $N_d = 1/\pi R^2$.

With a finite strain field, the dislocation acts as a

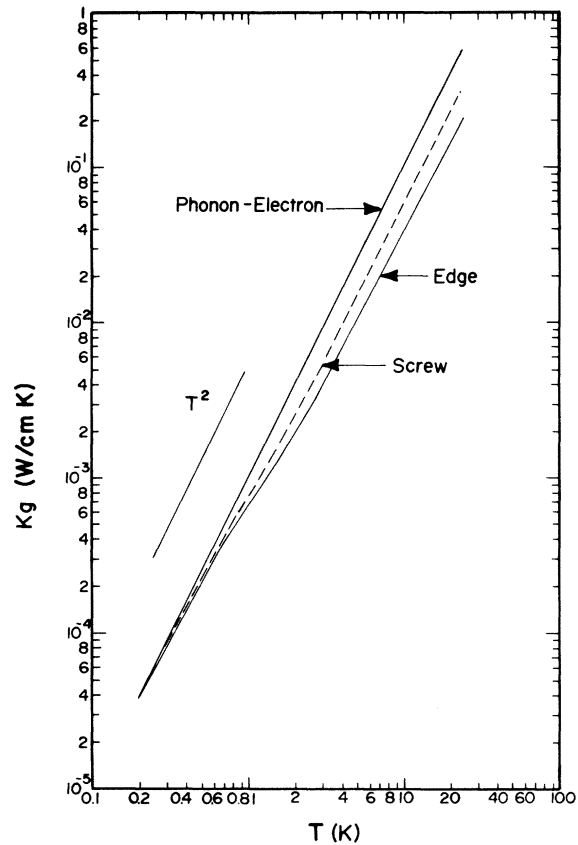


FIG. 3. Lattice thermal conductivity vs temperature for either all edge or all screw dislocations with finite strain fields. $N_E = N_S = 4.5 \times 10^{11} \text{ cm}^{-2}$.

cylindrical lens of varying index of refraction and radius R . When densities are small, R is large, and at all but the lowest temperatures, where phonon wavelengths are $\lambda \geq R$, scattering appears to be caused by an infinite strain field. The thermal conductivity curve can then be expected to exhibit very little structure, other than a T^2 behavior, which is what we find for $N_d = 4.5 \times 10^{10} \text{ cm}^{-2}$.

For an infinite strain-field-type scattering the condition $\lambda < R$ must be met. However, as the dislocation densities increase, this condition can only be satisfied at higher and higher temperatures. We thus would expect to see more structure in the thermal conductivity curves over a broader range of temperatures. Our curves corresponding to $N_d = 4.5 \times 10^{11} \text{ cm}^{-2}$ and $N_d = 9.0 \times 10^{11} \text{ cm}^{-2}$ illustrate this effect.

In Table I we attempt to lend more of a quantitative feel for the magnitude of this effect and the temperature range in which the transition from R to infinite strain-field scattering takes place. K_{ge}/K_g is the ratio of the lattice thermal conductivity limited by electrons alone to the lattice thermal conductivity with R field dislocation scattering included. The temperatures $T(10\%)$ and $T(50\%)$ are those at which K_g exceeds the lattice thermal conductivity in the limit of infinite strain-field scattering by 10% and 50%. In other words, where the ratio

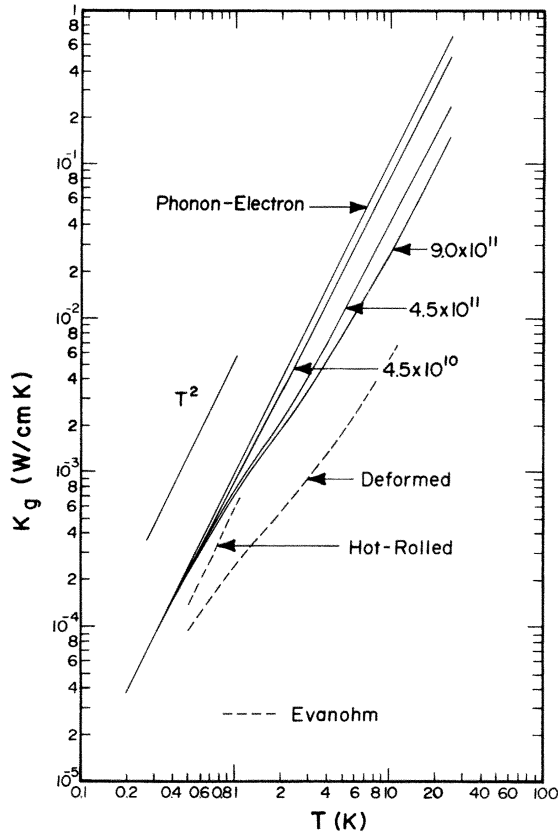


FIG. 4. Lattice thermal conductivity vs temperature for varying dislocation densities or, equivalently, for varying cutoff strain-field radii. Dislocation densities (in units of cm^{-2}) are indicated on the figure. Phonon-electron label stands for the phonon-electron-scattering-limited lattice thermal conductivity. The dashed curve is fitted to the experimental data of Linz *et al.* (Ref. 4) taken on heavily deformed Evanohm.

$K_g/K_{g\infty} = 1.1$ and 1.5 , respectively. The value of ΔT gives the temperature range in which the transition from 10% to 50% takes place.

Table I illustrates that which is predictably expected from the R field model. As the number of dislocations increases the ratio of K_{ge}/K_g increases, since R field scattering becomes stronger and more important. And, the temperature range in which transition from R to infinite

TABLE I. Temperatures at which K_g is 10% and 50% greater than $K_{g\infty}$.

K_{ge}/K_g at 3 K	N_d (10^{10} cm^{-2}) (edge and screw)	$T(10\%)$ (K)	$T(50\%)$ (K)	ΔT (K)
1.20	4.5	0.15	a	
1.33	9.0	0.30	b	
2.11	45	1.60	0.72	0.88
2.61	90	2.75	1.65	1.10
1.70	(45) ^c	2.10	0.65	1.45

^a $K_{ge}/K_{g\infty} = 1.12$, at 0.1 K $K_g \approx K_{ge}$.

^b $K_{ge}/K_{g\infty} = 1.21$, at 0.1 K $K_g \approx K_{ge}$.

^cScrew only.

strain-field scattering takes place also increases.

For comparison we display Table II, which is made up of the values from the earlier work of Ackerman and Klemens (AK).³ Several observations may be made. By comparing the number of dislocations for ratios of K_{ge}/K_g at 3 K we may conclude the AK calculation predicts a stronger interaction. In particular, in order to obtain the value of $K_{ge}/K_g = 2.1$ we had to increase the number of dislocations by an order of magnitude over AK to obtain the same value of this ratio. Also, it is apparent, by comparing values of ΔT , that our transitions from R to infinite strain-field scattering are more gentle, again reflecting the difference of the interaction strengths between the two calculations.

Finally, we have concluded that relative to our calculation the AK calculation overestimates the strength of the infinite strain-field scattering. One may determine this by observing that at lower dislocation densities our calculation yields values for the ratio $K_{ge}/K_{g\infty} < 1.5$ thus rendering it impossible for us to report values of $K_g/K_{g\infty} = 1.5$ as AK do ($K_{ge}/K_{g\infty}$ sets an upper bound on $K_g/K_{g\infty}$). Assuming that the electron-limited conductivities are approximately equal we would then have to decrease our $K_{g\infty}$ to obtain values of $K_{ge}/K_{g\infty} > 1.5$ and in turn to obtain $K_g/K_{g\infty} = 1.5$. We were unable to determine the magnitude of this overestimate since the AK paper reports only normalized values of thermal conductivity and temperature.

Another mechanism which would cut off the spatial extent of the strain field about a dislocation and reduce the scattering of long-wavelength phonons is the dislocation dipole—the pairing of parallel dislocations of opposite signs. Such pairing is much more restrictive than the assumption in the present model. While it could be an important mechanism which limits the spatial extent of the dislocation's strain field, such a restrictive assumption may be unnecessary in the formulation of a theory of the temperature dependence of lattice thermal conductivity at liquid-³He temperatures.

Grüner and Bross¹⁶ did propose such a dipole model. But, as AK point out, a comparison of the temperature dependence of the present model and theirs is complicated by the fact that Grüner and Bross used three-phonon N processes instead of phonon-electron interactions to prevent low-frequency divergence of the thermal conductivity integral. This may be proper in insulators at higher temperatures but in alloys at liquid-³He temperatures the dominant scattering mechanism is more likely the phonon-electron interaction.

TABLE II. Temperatures at which K_g is 10% and 50% greater than $K_{g\infty}$ taken from Ackerman and Klemens.

K_{ge}/K_g at 3 K	N_s (10^{10} cm^{-2}) (screw only)	$T(10\%)$ (K)	$T(50\%)$ (K)	ΔT (K)
2.1	4.5	0.63	0.29	0.34
3.0	8.2	1.10	0.53	0.57
4.0	12.0	1.52	0.77	0.75

More recently Brown¹⁷ has invoked the scattering by the static strain fields of edge dislocation dipoles to reconcile some of the discrepancies between the theory of Kneezel and Granato¹⁸ (KG) and the observations of Roth and Anderson¹⁹ in LiF. KG employed a dynamical model of scattering by narrow dipoles which resulted in a dislocation density of 30 times that which was obtained by etch pit measurements¹⁹ (which are themselves in question). Even though Brown's estimates complement the results of KG to give agreement between theory and experiment, he notes that in part the discrepancies above 2 K are probably due to scattering by point defects and three-phonon processes which were not included in the theory of KG. Since Brown only estimates the effects of the dipoles and never actually carries out a detailed calculation of K_g , and due to discrepancies that arose from the original theory of KG, we again find comparison with the present model's results difficult.

It appears then, that until a detailed calculation of the effects of dislocation dipoles on K_g is made for metallic alloy systems there is no clear and reliable way of comparing the two models. Also, even if the calculation is done the two mechanisms may be acting at the same time. Therefore, experimentally it would be very difficult to distinguish between the two,²⁰ thus obscuring verification of theoretical models.

Direct comparison of the results of the present calculation with experimental results on Cu-Al alloys below 1 K at this point does not seem to be possible. The reason is that good reliable lattice thermal conductivity data for this alloy system are not available.²⁰

Below 1 K, Anderson points out¹⁹⁻²¹ that measurements are difficult, and the extraction of K_g from K_{tot} more than likely will result in error, since the determination of K_e is in question. Specifically he points out that at such low temperatures the use of the Wiedemann-Franz law may be in question. The Wiedemann-Franz law is based on the thermodynamic absolute temperature scale, whereas K_{tot} is measured using a laboratory temperature scale. The laboratory temperature scale was based on the vapor pressure of liquid helium. And, what is more, the vapor-pressure scale itself was in error by an amount ranging from 0.2% at 5 K to possibly $\sim 1\%$ when extrapolated to $T < 0.1$ K.²² This situation was rectified by 1979 (Ref. 22) but all the data presently available on Cu-Al alloys were taken before that date.

Even above 1 K there is some disparity in the data. Anderson²² has collected and compared lattice thermal conductivity data from various laboratories.²³⁻²⁹ He shows that even though most laboratories are in agreement there are some cases in which differences as large as 2 orders of magnitude exist.²⁹

An additional complication which compounds the difficulty of comparing the results of the present model with experimental observation of Cu-Al alloys in the (1-3)-K range is the apparent presence of resonance scattering by fluttering dislocations. This appears as a bow in the K_g curve. The measurements of Linz *et al.*⁴ and Vorhaus and Anderson²¹ are in good agreement and show the bow between 2 and 3 K. Theoretically, as mentioned in the Introduction, the calculations of Madarasz and Klemens⁷ on resonance scattering by dislocations appear to have been successful in substantiating this mechanism. The com-

bined action of R field scattering and resonance scattering on K_g may look somewhat like the curve in Fig. 5. The dashed portions correspond to the data of Linz *et al.*⁴ on Cu-10 at. % Al.

Because of the problems with Cu-Al data mentioned above we are unable to make a direct comparison between the present theoretical model's results and experimental observations. Evanohm, on the other hand, exhibits none of these problems. Experimental data indicate little or no resonance scattering taking place. Furthermore, as mentioned in the Introduction, it has a very high residual resistivity and thus possesses a small electronic component of thermal conductivity. By virtue of this fact, extraction of K_g from K_{tot} can be achieved with a higher degree of accuracy than, for instance, in Cu-Al alloys.

In principle the differences between a calculation of the effects of R field scattering on K_g for Cu-Al versus Evanohm are small. For low temperatures these differences lie mainly in the strength of phonon-electron scattering and in the lattice constant. The Debye temperature and impurity scattering become more significant at higher temperatures beyond where R field scattering is expected to be important. In light of these facts and those mentioned above concerning Cu-Al alloys, we find it reasonable to compare our results with the data on Evanohm. We do so in Fig. 4 where the dashed curve fits the experimental data of Linz *et al.*⁴ for Evanohm. The reported number of dislocations in the deformed Evanohm was in excess of 10^{11} cm⁻². As can be seen, the temperature dependence is very similar to that calculated in the

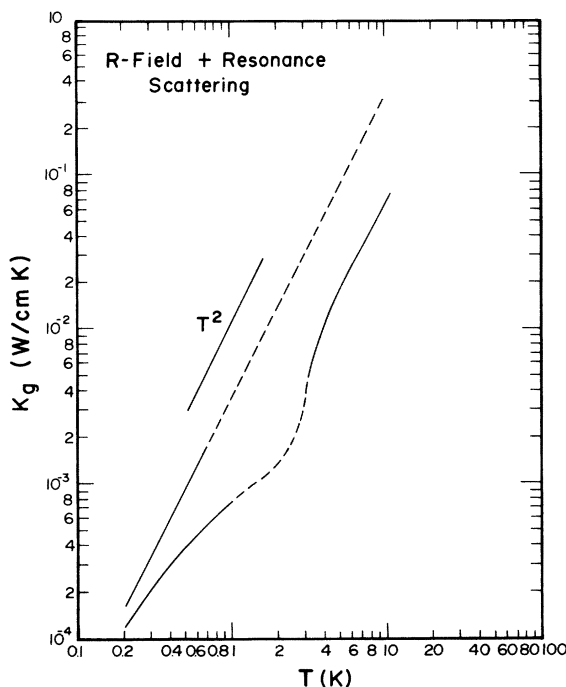


FIG. 5. Estimated lattice thermal conductivity vs temperature when both finite strain-field and resonance scattering are present. The dashed portions are fitted to the data of Linz *et al.* (Ref. 4) taken on well-annealed and heavily deformed Cu-10 at. % Al.

theoretical curves. We also note that the lower displacement of K_g is indeed due to a stronger phonon-electron interaction. Should the Evanohm curve be normalized to the Cu-Al electron-limited conductivity curve it would fall very close to the theoretical curves and in the proper range of dislocation densities.

IV. SUMMARY

The original calculation of phonon scattering by a limited strain field around a screw dislocation due to Ackerman and Klemens was amended to account for the two dimensionality of the problem. The model was also extended to include phonon-edge dislocation interactions. An additional feature in our work was the averaging of the projection of the phonon's wave vector onto the xy plane in which the scattering takes place. For the case of an edge dislocation, scattering was dependent on the angle between the strain-field position vector $\vec{\rho}$ and the scattering vector \vec{Q}' . This angular dependence was averaged as well.

The theory of phonon scattering by a finite dislocation strain field was then applied to the problem of lattice thermal conductivity in copper alloys. At the lower temperatures, where phonon wavelengths are large compared to the cutoff radius, dislocation scattering was found to be weak. The thermal conductivity curves reflected the dominance of the phonon-electron scattering. As temperature was increased, phonon wavelengths became comparable to and less than the cutoff radius. Owing to this, the thermal conductivity curves exhibited more structure bending to-

ward a T^2 dependence, which is what is expected for infinite strain-field scattering.

In the temperature regime where R field scattering is expected to be important, a comparison with experimental data on Cu-Al alloys was not possible. The difficulties in making the comparison were twofold. First, below 1 K there is no reliable data. Second, above 1 K, to about 3 K, an additional scattering mechanism, resonance scattering, acts, which tends to obscure the identification of the effects of the R field scattering. Comparison with the experimental data on the commercial alloy Evanohm was, however, possible. Being of high residual resistance, the extraction of K_g from K_{tot} in Evanohm is effectively devoid of the problems found with most other metallic alloys, in particular Cu-Al. Furthermore, resonance scattering is apparently damped out. Thus over the range of temperatures where R field scattering is expected to occur Evanohm does indeed appear to be a reliable source for comparison. The temperature dependence of our thermal conductivity curves has been found to be very similar to what is seen in Evanohm.

ACKNOWLEDGMENTS

We are especially indebted to Dr. P. G. Klemens for many helpful discussions and his critical review of the manuscript. His encouragement throughout the course of the work was greatly appreciated. Also we would like to thank Dr. A. C. Anderson for a very helpful discussion on the difficulties concerned with obtaining data at very low temperatures.

¹U. F. Kocks and R. O. Scattergood, *Acta Metall.* **17**, 1161 (1958).

²P. G. Klemens, in *Solid State Physics*, edited by F. Seitz and D. Turnbull (Academic, New York, 1958), Vol. 7, p. 1.

³M. W. Ackerman and P. G. Klemens, *Phys. Rev. B* **3**, 2375 (1971).

⁴R. J. Linz, T. K. Chu, A. C. Bouley, F. P. Lipschultz, and P. G. Klemens, *Phys. Rev. B* **10**, 4869 (1974).

⁵A. C. Anderson (private communication).

⁶D. H. Damon and P. G. Klemens (private communication).

⁷F. L. Madarasz and P. G. Klemens, *Phys. Rev. B* **23**, 2553 (1981).

⁸J. M. Ziman, *Electrons and Phonons* (Clarendon, Oxford, 1960), pp. 229–231, 353–355.

⁹F. R. N. Nabarro, *Theory of Crystal Dislocations* (Clarendon, Oxford, 1967), pp. 56 and 57.

¹⁰We would like to point out that in Ziman's treatment (Ref. 8) of phonon scattering by an infinite strain field about a screw dislocation his expression (6.4.5), which corresponds to our Eq. (2.6), contains in it a factor of $\frac{1}{2}$. Our equation contains $\frac{1}{4}$. This results in his differential scattering width being a factor of 2 larger than ours. A reason for this may be that since the strain tensor is symmetric there are two off-diagonal elements contributing equally to the scattering process. He may then have multiplied the transition element by 2 to take this into account. We feel that our procedure, as given in the text, of multiplying the square of the transition element by 2, is the

correct one.

¹¹Equations (2.20) and (2.21) for transition rates contain no transition elements due to cross terms in strain. In the present model no distinction is made between polarization branches, and for phonon velocities we use their spherically averaged values. In this type of approximation, phase information is lost and cross terms vanish. P. G. Klemens, *Proc. Phys. Soc. London Sect. A* **12**, 1113 (1955).

¹²P. Carruthers, *Rev. Mod. Phys.* **33**, 92 (1961).

¹³J. W. Mitchell, J. C. Cherrier, B. J. Hockey, and J. P. Monaghan, Jr., *Can. J. Phys.* **45**, 453 (1967).

¹⁴P. G. Klemens, *J. Appl. Phys.* **39**, 5304 (1968).

¹⁵M. A. Mitchell, P. G. Klemens, and C. A. Reynolds, *Phys. Rev. B* **3**, 1119 (1971).

¹⁶P. Grüner and H. Bross, *Phys. Rev.* **172**, 583 (1968).

¹⁷R. A. Brown, *Solid State Commun.* **42**, 847 (1982).

¹⁸G. A. Kneezel and A. V. Granato, in *Proceedings of the Acta/Scripta Metall. International Conference on Dislocation Modelling of Physical Systems*, Gainesville, 1980 [*Phys. Rev. B* **25**, 2851 (1982)].

¹⁹E. P. Roth and A. C. Anderson, *Phys. Rev. B* **20**, 768 (1979).

²⁰A. C. Anderson (private communication).

²¹J. L. Vorhaus and A. C. Anderson, *Phys. Rev. B* **14**, 3256 (1976).

²²A. C. Anderson, in *Dislocations in Solids*, edited by F. R. N. Nabarro (North-Holland, Amsterdam, in press).

²³W. R. G. Kemp, P. G. Klemens, and R. J. Tarnish, *Philos.*

- Mag. 4, 845 (1959).
- ²⁴J. N. Lomer and H. M. Rosenberg, *Philos. Mag.* 4, 467 (1959).
- ²⁵P. Charsley, J. A. M. Salter, and A. D. W. Leaver, *Phys. Status Solidi* 25, 531 (1968).
- ²⁶Y. Kogure and Y. Hiki, *J. Phys. Soc. Jpn.* 32, 698 (1975).
- ²⁷R. Zeyfang, *Phys. Status Solidi* 24, 221 (1967).
- ²⁸R. W. Klaffky, N. S. Mohan, and D. H. Damon, *Phys. Rev. B* 11, 1297 (1975).
- ²⁹M. Kusunoki and H. Suzuki, *J. Phys. Soc. Jpn.* 26, 932 (1969).